Carbon-11 acetate as a tracer of myocardial oxygen consumption

Lucas J. Klein[1], Frans C. Visser[1], Paul Knaapen[1], Job H. Peters[1], Gerrit J.J. Teule[2], Cees A. Visser[1], Adriaan A. Lammertsma[2]

[1] Department of Cardiology, University Hospital VU, P.O. Box 7057, 1007 MB Amsterdam, The Netherlands
[2] Clinical PET Centre, University Hospital VU, Amsterdam, The Netherlands

Published online: 6 March 2001
© Springer-Verlag 2001

Abstract. Estimation of myocardial oxygen consumption (MVO_2) and myocardial blood flow (MBF) is important for the understanding of various (patho)physiological mechanisms and diseases. Clearance rates of carbon-11 labelled acetate, determined with positron emission tomography, allow estimation of MVO_2 on a segmental level and non-invasively. In addition, MBF can be determined from uptake rates. In this review, the background to estimation of MVO_2 and MBF is discussed, as well as the currently available literature that has used ^{11}C-acetate to estimate MVO_2 and MBF.

Keywords: Myocardial oxygen consumption – Myocardial blood flow – Carbon-11 acetate – Positron emission tomography

Eur J Nucl Med (2001) 28:651–668
DOI 10.1007/s002590000472

Introduction

The heart relies almost exclusively on aerobic oxidation of substrates for the generation of ATP, which is required to maintain its contractile function. In the normal heart, oxygen demand is in balance with oxygen supply, which is determined by myocardial blood flow and oxygen extraction. Though myocardial oxygen extraction is high at rest in normal subjects (~70%) [1], there is considerable variation at pacing induced exercise [1, 2], in coronary artery disease [3, 4] and in other types of patients [5, 6, 7]. Also, in many disease processes the balance between demand and supply is disturbed. For a better understanding of the pathophysiology, and possibly for improved evaluation of therapies, it is important to measure not only perfusion but also myocardial oxygen consumption (MVO_2), in particular at a regional level.

With the introduction of positron emission tomography (PET), a number of tracers have been developed for the quantification of regional substrate metabolism and perfusion. Over the past two decades, various studies have demonstrated that PET with ^{11}C-acetate provides an accurate estimate of MVO_2 and perfusion. In this review, the background, validation and applications of ^{11}C-acetate as a tracer of MVO_2 and perfusion will be discussed.

Lucas J. Klein (✉)
Department of Cardiology, University Hospital VU,
P.O. Box 7057, 1007 MB Amsterdam, The Netherlands
e-mail: lj.klein@azvu.nl
Tel.: +31-20-4442244, Fax: +31-20-4442446

Determinants and measurement of MVO_2

Determinants of MVO_2

MVO_2 can be divided into two components: oxygen required for contraction (work) and oxygen required for the other processes in cardiac cells, e.g. electrical conduction and basal metabolism. Braunwald defined nine determinants of MVO_2 (Table 1) [8]. The three major determinants of MVO_2 are tension development, contractility and heart rate. When the heart is arrested with potassium chloride in dogs, MVO_2 falls from 8–15 ml O_2/100 g per minute in the contracting heart to 2 ml O_2/100 g per minute [9]. This amount of oxygen is required for processes not directly related to contraction. The energy costs required for electrical activation are very small, accounting for 0.5% of total MVO_2 in the normal working heart [10]. Other factors, such as the metabolic effects of catecholamines and the maintenance of the active state, are less important [8].

In fact, these determinants of MVO_2 are determinants of the ATP requirement. It is thereby assumed that the ATP requirement is identical to the oxygen requirement. However, this assumption is not correct, as will be explained later in this review.

Table 1. Determinants of MVO_2 according to Braunwald [8]

Tension development
Contractile state
Heart rate
Basal cost
Depolarisation
Direct metabolic effect of catecholamines
Activation
Maintenance of active state
Shortening against a load – Fenn effect

Table 2. Determination of MVO_2

I. Global	
Direct:	Measurement of myocardial O_2 consumption Arterial-venous oxygen difference multiplied by flow
Indirect:	Measures of oxygen demand Rate-pressure product [14] Triple product [15] Tension-time index [16] Pressure-work index [17] Velocity of shortening [18] Circumferential wall stress [19] Bretschneider index [20] Pressure-volume area [21]
II. Regional	
PET-derived methods:	^{11}C-acetate Oxygen extraction fraction multiplied by flow

Measurement of MVO_2

MVO_2 can be measured both directly and indirectly. The direct method requires arterial and venous catheterisation. The venous catheter is used to measure oxygen saturation and myocardial blood flow (MBF) in the coronary sinus. Using the Fick principle [11, 12], the MVO_2 of the heart as a whole can be calculated by the arterial-venous oxygen difference multiplied by MBF [5, 13]. This method has the drawback of positioning difficulties within the coronary sinus [5] and variation in myocardial venous drainage [4], with possible errors in either the determination of MBF or in oxygen content of the blood. Although only global MVO_2 can be determined, it is still the gold standard.

Because of the invasive nature of the direct method, various indices of MVO_2 have been developed based on the major determinants of oxygen demand (Table 2). Examples are the rate-pressure product (RPP), wall stress, pressure-work index, pressure-volume area, triple product and other indices [14, 15, 16, 17, 18, 19, 20, 21, 22, 23, 24]. The RPP is often used because of its good correlation with MVO_2 in the normal human heart [14, 20, 22, 23]. Whilst these indices are adequate as an index of MVO_2 in the normal heart, they are possibly less reliable in the diseased state. In addition, they only provide information on global MVO_2.

Other indirect methods are provided by radiotracer techniques. Of the available tracers of metabolism that can be labelled with positron emitters, carbon-11 acetate and oxygen-15-labelled oxygen are suitable for measuring MVO_2. ^{15}O-oxygen can be used to measure MVO_2 directly [25, 26, 27]. Estimation of MVO_2 with ^{11}C-acetate is discussed in this review. The advantages of these radiotracer techniques are that they are non-invasive and, more importantly, that they provide information at a regional level.

Rationale of using labelled acetate as a tracer of MVO_2

Oxidative phosphorylation

ATP is produced by either substrate-level or oxidative phosphorylation of ADP. The contribution of substrate-level phosphorylation to total ATP production is small. Oxidative phosphorylation is the process in which electrons are transferred from reducing equivalents to oxygen by a chain of electron carriers, producing water in the final step. It is the principal mechanism of oxygen usage in the cell, and the only mechanism present in myocardium. Therefore, MVO_2 is identical to flux through oxidative phosphorylation.

The reducing equivalents used in oxidative phosphorylation are NADH + H^+ and $FADH_2$. Both carry electrons from processes in the tricarboxylic acid cycle (TCA cycle), glycolysis and beta-oxidation, as depicted in Fig. 1. The ratio between reducing equivalents derived from the TCA cycle and those derived from glycolysis and beta-oxidation is fairly stable, with a ratio of approximately 2:1 in favour of the TCA cycle. Consequently, about two-thirds of the oxygen used in the cell is used for reducing equivalents derived from the TCA cycle. The ratio is dependent on the chain length of the fatty acids used by the cell. In mammals, mainly chains with lengths of 16 and 18 C atoms are used [28], resulting in a maximum change in the ratio of 6%.

Acetate, a free fatty acid (FFA) with a chain length of two, enters the TCA cycle directly after conversion to acetyl-CoA. Further metabolism of acetate is described in the next section. Because of the direct entry in the TCA cycle, labelled acetate can be used to measure the flux of the TCA cycle and thus of the production of reducing equivalents. As this is tightly coupled to oxygen consumption, the latter can be estimated by measuring the flux through the TCA cycle with acetate.

Although the ratio of the number of reducing equivalents derived from the TCA cycle and glycolysis and beta-oxidation is fairly stable, there is a difference in ATP production per molecule of oxygen used. The ATP yield of $FADH_2$ is two instead of three because it enters oxida-

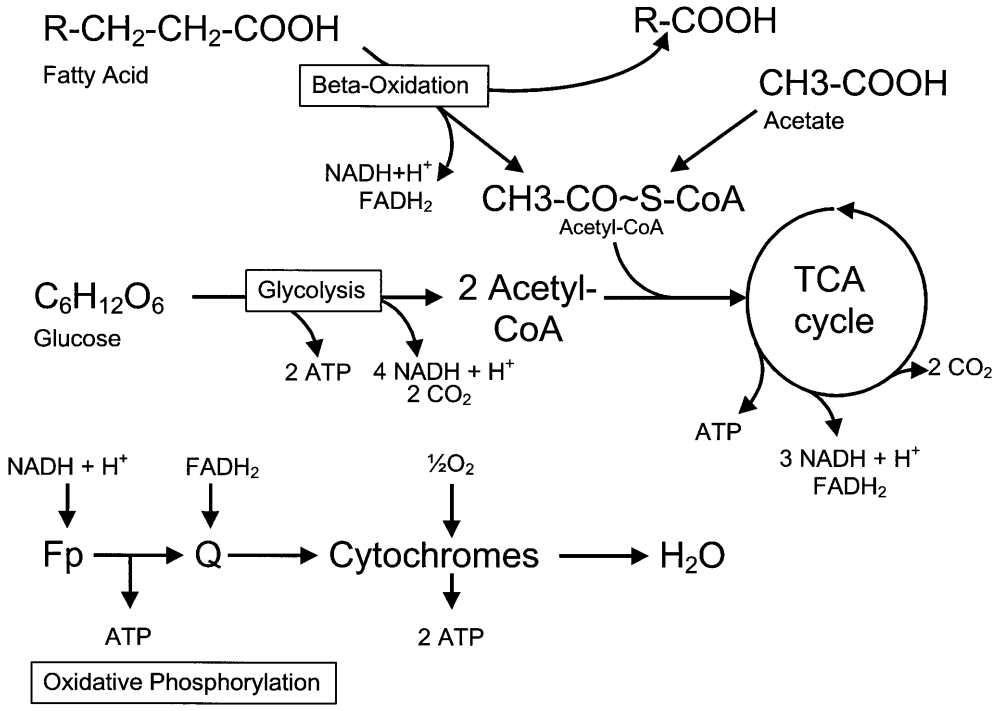

Fig. 1. Oxidative metabolism in cells. NADH + H^+ and $FADH_2$ are produced by several processes, including glycolysis, beta-oxidation and the oxidation of acetyl-CoA. Glycolysis produces two acetyl-CoA for entrance in the TCA cycle. Acetate enters the cycle after conversion to acetyl-CoA. NADH + H^+ and $FADH_2$ are oxidised by oxidative phosphorylation (located in the mitochondrial membranes) with the generation of three and two ATP, respectively. From this figure, one can calculate the ATP yield and oxygen cost for glucose, acetate and other fatty acids. Not shown in the figure is the initial activation of acetate and FFA, with the conversion of ATP to AMP. *NADH + H^+*, Nicotinamide adenine dinucleotide (reduced); *$FADH_2$*, flavin adenine dinucleotide (reduced); *Fp*, flavoprotein; *Q*, coenzyme Q; *TCA cycle*, tricarboxylic acid cycle

tive phosphorylation later than NADH + H^+ (Fig. 1). Furthermore, glycolysis has substrate-level phosphorylation (two ATP net yield), whereas beta-oxidation has not. Activation of FFA (coupling of co-enzyme-A to FFA) even costs two ATP. From Fig. 1, one can calculate for various substrates the number of reducing equivalents and ATP molecules produced as well as the number of oxygen molecules used. For example, one glucose (6 C atoms) produces 10 NADH + H^+, 2 $FADH_2$ and 38 ATP with the use of six molecules of oxygen. Eight (67%) of the reducing equivalents are derived from the TCA cycle. Palmitate (16 C atoms) produces 31 NADH + H^+, 15 $FADH_2$ and 129 ATP with the use of 23 molecules of oxygen. Thirty-two (70%) of the reducing equivalents are derived from the TCA cycle. These numbers include the substrate-level phosphorylation and the activation of the fatty acid. A complete transition from glucose to palmitate as fuel will change the ratio between the number of reducing equivalents derived from the TCA cycle by about 3%. However, the ratio of the number of ATPs produced per molecule of oxygen changes from 6.33 to 5.61, a change of 13%. Thus, with the same workload and thus ATP requirement, the transition will result in an increase in MVO_2 by about 13%. This increase is even greater when FFAs with a shorter chain length are available.

The above implies that metabolic standardisation is not necessary for measurement of MVO_2 with ^{11}C-acetate itself, but becomes important when such measurements are related to haemodynamic indices. This is true not only for measurements with ^{11}C-acetate, but also for other measurements of MVO_2 that are related to haemodynamic indices.

Metabolic pathway of acetate labelled in the C-1 position

The metabolic fate of acetate labelled in the carboxyl (C-1) position [(C-1)acetate] in myocardium is depicted in Fig. 2. Extraction of acetate by myocardium is high and once transported into the cell, (C-1)acetate is converted to (C-1)acetyl-CoA by acetyl-CoA synthetase in the mitochondrial matrix [29]. (C-1)acetate has no other major metabolic pathways in the myocardium [30]. (C-1)acetyl-CoA is readily oxidised via the TCA cycle, which can be divided into two cycle turns. First, (C-1)acetyl-CoA condenses with oxalo-acetate to form (C-5)citrate. (C-5)citrate converts into (C-5)α-ketoglutarate, which equilibrates very rapidly with (C-5)glutamate [30, 31, 32]. In the final step of the first cycle turn (C-1 or C-4)oxaloacetate (the labelled carbon atom can be in either position) is formed, which also equilibrates quickly with (C-1 or C-4)aspartate [31]. Two molecules of CO_2

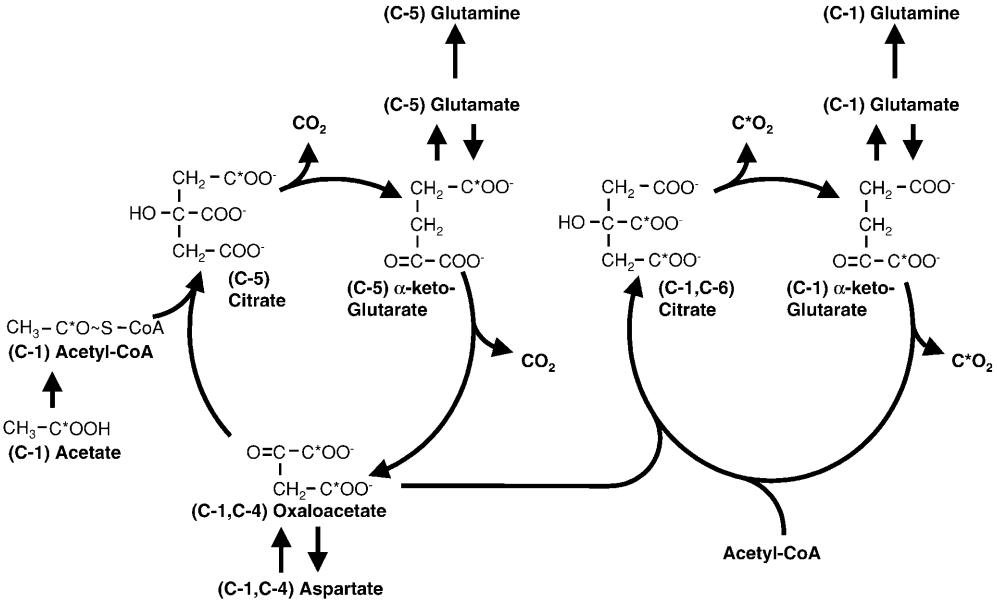

Fig. 2. Metabolic pathway of acetate labelled in the C-1 position. C-*n* and * denote where the label resides in the various intermediate products. When * appears twice in a molecule, the label can reside in either position. See text for further explanation

are released in the first cycle turn; however, none of the carbon atoms are from the C-1 position and therefore are not labelled.

(C-1 or C-4)oxaloacetate from the first turn condenses with acetyl-CoA to form (C-1 or C-6)citrate and thus initiates the second TCA cycle turn. Decarboxylation of (C-1 or C-6)citrate, with the release of CO_2, which is labelled when the C-6 atom is labelled, forms (C-1)α-ketoglutarate, which again equilibrates rapidly with (C-1)glutamate [30, 31, 32]. Decarboxylation of (C-1)α-ketoglutarate releases the final labelled molecule of CO_2. Thus, in this second cycle-turn, the labelled C atoms are released as labelled CO_2 (or bicarbonate in tissue). It is generally assumed that this labelled bicarbonate leaves the tissue rapidly.

Because acetate has no other pathways for metabolism in the myocardium, it can be used to estimate TCA cycle flux and thus MVO_2. Although there is a rapid conversion to amino acids such as glutamate and aspartate, these intermediates are mainly taken up again in the cycle. The exchange rate between α-ketoglutarate and glutamate was found to be more than 10 times higher than the rate of the TCA cycle [31]. Glutamate can also be converted to glutamine, a slow and almost irreversible process [32, 33]. Although glutamine may leave the cycle, back-conversion from glutamate to α-ketoglutarate is much faster than the irreversible conversion to glutamine [32]. Therefore, the labelled glutamine pool will be very small and can probably be neglected [32].

Validation of the use of ^{11}C-acetate for determination of MVO_2

First publications of ^{11}C-acetate production and the use in dogs and humans date back to the early 1980s [34, 35, 36, 37]. Acetate clearance in humans was similar to that in dogs and clearance from myocardium rendered ischaemic was slower than that from remote normal myocardium [34, 35, 37]. Clearance during exercise and pacing was enhanced, but was not significantly faster when MBF was increased by 90% with dipyridamole [36]. These initial results led to investigations into the usage and validation of ^{11}C-acetate as a tracer of MVO_2.

Direct comparison of acetate clearance and MVO_2

Brown et al. demonstrated in isolated, perfused rabbit hearts that the time-activity curve of $^{14}CO_2$ in the venous effluent of the heart after 2 min perfusion with ^{14}C-acetate was bi-exponential [38]. The fast clearance rate of $^{14}CO_2$ in the venous effluent correlated closely with MVO_2. The efflux of activity consisted almost completely of $^{14}CO_2$ after 3 min, indicating that back-diffusion of tracer and leakage of labelled metabolites other than CO_2 from the heart was minimal. When ^{11}C-acetate was coinjected, the externally detected myocardial time-activity curve (with NaI detectors in a coincidence circuit) showed a similar bi-exponential clearance. Mono-exponential clearance was seen in ischaemia and hypoxia. These conditions were accompanied by a lower heart rate and lower blood pressure. Steady-state extraction of ^{14}C-acetate was ~60% in normoxia, increasing to ~93% in ischaemia. Ketone production and incorporation into lipids were low, even in ischaemic hearts. Similar results were obtained by Buxton et al. in isolated perfused rat hearts [30]. Peak efflux occurred 3.0±0.8 min after bolus injection of the tracer. Labelled CO_2 accounted for ~97% of the total ^{14}C activity in the effluent of the heart between 10 and 20 min after intracoronary injection.

Armbrecht et al. determined clearance rates of ^{11}C-acetate measured with a gamma probe in the left anteri-

or descending artery (LAD) territory of hearts of open-chest dogs [33]. Single-pass extraction fraction was high in normoxia, in ischaemia and at increased workload (60%–70%), but was significantly decreased to ~47% in dipyridamole studies. Clearance of acetate showed a close correlation with measured MVO_2 when fitted with either a mono- or a bi-exponential in all conditions; it was also closely correlated with myocardial blood flow, except in dipyridamole studies. In studies using simultaneous injection of ^{11}C- and ^{14}C-acetate, the fraction of $^{14}CO_2$ activity contributing to total ^{14}C activity leaving the heart was high in all conditions, varying from ~89% in ischaemia to >99% in dipyridamole studies. Clearance of $^{14}CO_2$ measured in the coronary effluent was identical to externally measured clearance of ^{11}C-acetate.

Direct comparison of ^{11}C-acetate clearance measured with PET and MVO_2

Brown et al. demonstrated a close correlation between myocardial ^{11}C-acetate clearance and MVO_2 in closed-chest dogs under various workloads [39, 40]. Furthermore, ^{11}C-acetate clearance was closely correlated with the RPP [39]. Clearance of ^{11}C-acetate from the myocardium was bi-exponential [39, 40], and was similar to $^{11}CO_2$ clearance in the coronary sinus [39]. Buxton et al. observed that bi-exponential clearance rates were closely correlated with measured MVO_2 and with mono-exponential clearance rates, suggesting that time-activity curves can also be fitted with a mono-exponential when fitting with a bi-exponential is difficult [41]. Sun et al. correlated clearance rates with invasively measured MVO_2 in humans, but obtained reasonable correlations at best (r=0.71 for mono-exponential fitting and r=0.73 for bi-exponential fitting) [42]. An explanation could be that subjects were only studied at rest, with narrow ranges of MBF and MVO_2.

Schulz et al. studied pigs early (acquisition 5–45 min) and late (acquisition 60–90 min) after MBF reduction to 50% [43]. Myocardial time-activity curves were fitted with a mono-exponential and related to measured MVO_2. Initially after flow reduction, clearance was reduced in concordance with MVO_2, but clearance recovered without a concordant increase in MVO_2 late after flow reduction. The results were explained by reduced concentrations of glutamate and aspartate in the myocardium (determined from biopsies) under prolonged ischaemia. Correction of clearance rates for these reduced concentrations restored the relationship with MVO_2, suggesting that reduction in the pool sizes of aspartate and glutamate is primarily responsible for the recovery of acetate clearance. Remarkable were the high mono-exponential clearance rates reported, in combination with the low concentrations of glutamate and aspartate in myocardium compared to other studies.

Relation between ^{11}C-acetate clearance and RPP in humans

A number of authors have studied subjects at rest and under dobutamine stimulation [44, 45, 46, 47]. Henes et al. [44] observed mono-exponential clearance of ^{11}C-acetate at rest, which became bi-exponential under dobutamine stimulation. The clearance rates from the mono-exponential fit as well as the fast clearance rate of the bi-exponential fit were used in a single linear regression analysis, which showed a close correlation between clearance rates and the RPP. Krivokapich et al. [45] and Tamaki et al. [46, 47] fitted curves only with a mono-exponential, and a close correlation between mono-exponential clearance and the RPP was reported. Armbrecht et al. observed biphasic curves both at rest and with supine bicycle exercise [48]. Both mono- and bi-exponential curve fits showed a close correlation with the RPP.

Vanoverschelde et al. correlated several oxygen consumption indices with MVO_2 calculated from the mono-exponential clearance rate of ^{11}C-acetate [49], based on the linear relation between clearance and MVO_2 obtained in dogs by Armbrecht et al. [33]. MVO_2 was best correlated to the pressure-volume area (r=0.92) and pressure-work index (r=0.92), followed by RPP (r=0.87). Administration of dobutamine decreased myocardial efficiency. It was also suggested that the RPP is a less adequate parameter to use for the correlation between MVO_2 and cardiac work, mainly because the change in RPP was not very well correlated with the change in MVO_2.

Porenta et al. used data obtained from both gated and dynamic acquisitions after injection of ^{11}C-acetate, during rest and dobutamine infusion [50]. MVO_2 (mono-exponential curve fitting) and MBF were both measured with ^{11}C-acetate. Gated acquisition was used to determine parameters that can be used to calculate tension-area area, an extension of the pressure-volume area. Stepwise linear regression analysis demonstrated that the RPP and external work together correlated significantly with MVO_2. Oxygen extraction increased during dobutamine infusion (from 59%±8% to 76%±9%). Mechanical efficiency did not change, while external work efficiency increased during dobutamine infusion.

The regression data regarding the relation between mono-exponential and bi-exponential curve fitting and the RPP that have been reported are shown in Table 3. Despite the fact that close correlations were reported, the range of slopes is rather large, for both mono- and bi-exponential fitting procedures. The reason for this is unclear. It may be due to variations in study conditions, the subjects studied or other factors. Too few studies have reported full data sets to combine those studies to obtain a lumped slope and intercept.

Table 3. Relation of mono-exponential and bi-exponential curve fits with the RPP: results from linear regression analysis

Authors	Subjects	No. of exp.	Mono-exponential fitting			Bi-exponential fitting		
			Slope ($\times 10^{-6}$)	Intercept	Corr. coeff.	Slope ($\times 10^{-6}$)	Intercept	Corr. coeff.
Brown et al. [39]	Dogs	14				10.4	–0.005	0.95
Henes et al. [44]	Dogs	36				8.3	0.022	0.88
Brown et al. [40]	Dogs	22				6.2	0.054	0.84
Armbrecht et al. [48]	Humans	22	5.89	0.014	0.91	11.5	–0.016	0.95
Henes et al. [44]	Humans	14				12.5	0.025	0.91
Tamaki et al. [47]	Humans	18	6.82	0.014	0.87			
Tamaki et al. [46]	Humans	28	6.72	0.013	0.86			
Krivokapich et al. [45]	Humans	22	8.50	–0.007	0.94			
Vanoverschelde et al. [49][a]	Humans	16	5.14	0.022	0.87	10.5	–0.014	0.83

No. of exp., Number of experiments; Corr. coeff., correlation coefficient
[a] Figures calculated from data provided in the original publication

Modelling of acetate kinetics

The initial studies validating acetate as a tracer of MVO_2 all applied simple mono- or bi-exponential curve fitting procedures to correlate clearance rates with MVO_2 or an index of MVO_2. This method is easy to apply but does not account for the arterial input function or the uptake of acetate by the myocardium, and it neglects pool sizes. In addition, corrections for spillover, partial volume and blood volume are not possible. To address these problems, various authors have investigated models of acetate kinetics.

Buck et al. investigated two- and one-tissue compartment models (Fig. 3) [51]. Curve fitting by the model included estimation of spillover from the cavity and from myocardial blood volume. The arterial input function was corrected for circulating labelled ^{11}C-CO_2. In closed-chest dogs, model-fitted clearance (k_2 from model A in Fig. 3) and directly measured MVO_2 were closely correlated (r=0.94). Curve fits were significantly tighter when correction for circulating ^{11}C-CO_2 was applied. ^{11}C-CO_2 accumulated rapidly in blood and, after 10 min, equilibrated at approximately 65% and 90% of the total activity in blood in dogs and humans, respectively. The formation of ^{11}C-CO_2 and other labelled metabolites could be described with a relatively simple function. Studies in humans using the simpler models (B and C from Fig. 3) showed a close correlation between model-fitted clearance and the RPP (r=0.91), compared with 0.61 for conventional mono-exponential curve fitting. However, those studies were only performed at rest. The simple model C in Fig. 3 was also investigated by Raylman et al. [52]. Corrections for circulating ^{11}C activity were made by simultaneous fitting of time-activity curves from eight myocardial ROIs using common parameters to account for metabolites and ^{11}C-CO_2. This method was investigated in five patients with idiopathic dilated cardiomyopathy studied at baseline and with low-dose dobutamine infusion. Clearance rates determined by this method were closely correlated with measured MVO_2 (r=0.85) in five patients with dilated cardiomyopathy and were better than when the eight curves were fitted independently (r=0.77).

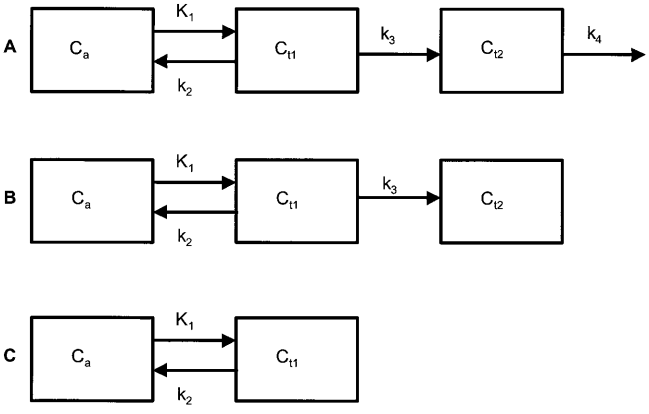

Fig. 3. Compartment models used by several authors [51, 52, 53, 55]. C_a represents arterial, and C_{t1} and C_{t2} tissue compartment ^{11}C-acetate activities. Rate k_2 is the rate that is correlated with MVO_2 or the RPP. K_1 denotes the uptake rate of the tracer into the tissue, k_3 transport of the label between tissue compartments, and k_2 and k_4 transport of the label from tissue to blood

Wolpers et al. used a two-tissue compartment model (model B of Fig. 3) [53]. The arterial input function was determined from rapidly drawn blood samples and not corrected for ^{11}C-CO_2 or other metabolites. Thirty-six experiments in 12 dogs were performed, with four different interventions to alter haemodynamic states. Modelled clearance of acetate was closely correlated to the additive index of Bretschneider (E_t) [20] (r=0.95). Correlation with the RPP was 0.88.

Ng et al. formulated a six-tissue compartment model (Fig. 4), which was developed to eventually calculate MVO_2 [32]. The model was investigated with ^{14}C- and

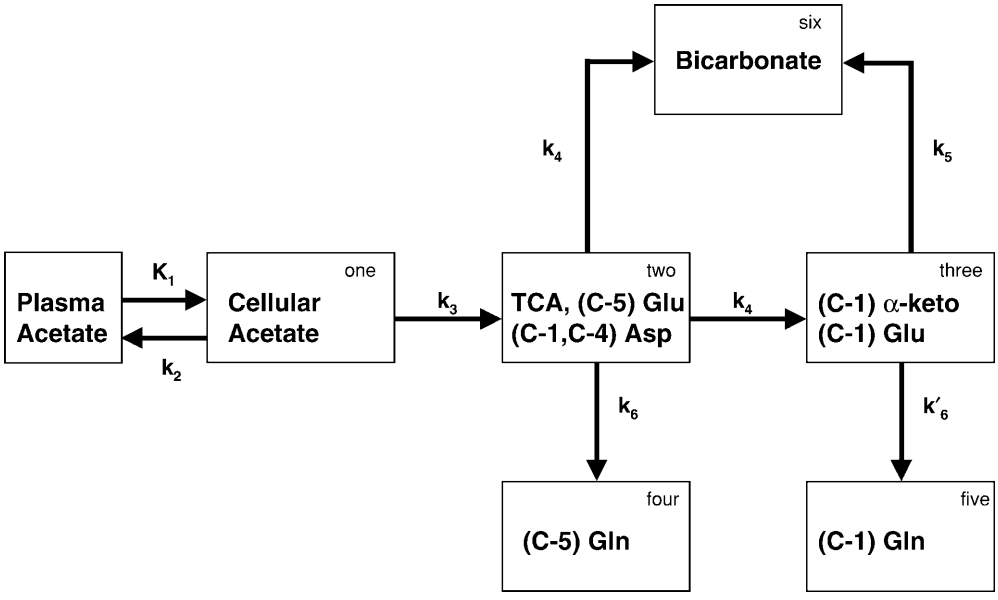

Fig. 4. Six-tissue compartment model used by Ng et al. [32]. Acetate enters the cell from the plasma by rate K_1 and diffuses back by rate k_2. Compartments two and three represent the first and second cycle turns, respectively (see also Fig. 2). Compartments four and five represent glutamine. Formation of bicarbonate (equivalent to CO_2) is by rate k_4 and k_5. Rate k_4 appears twice because CO_2 and the substrate for the second cycle turn are formed at the same rate. Rates k_4 and k_5 are said to be identical. Glutamine formation is by rate k_6 and considered irreversible. *TCA*, Tricarboxylic acid cycle; *Glu*, glutamate; *Asp*, aspartate; *Gln*, glutamine; *α-keto*, α-ketoglutarate

^{11}C-acetate in crystalloid perfused rat hearts. The extraction fraction was determined from externally measured time-activity curves using ^{11}C-acetate. Tissue concentrations of glutamate, aspartate, glutamine and TCA cycle intermediates were determined in a number of hearts 2, 5, 10, 20 and 40 min post injection. Concentrations of glutamate and aspartate were found to be approximately eight times higher than concentrations of TCA cycle intermediates in normoxia, but only 4.7 times higher in ischaemia. Two minutes after injection, the majority of the label was found in glutamate. The contribution of (C-1)glutamate (derived from the second cycle turn) to total tissue radioactivity was markedly delayed in hypoxia and ischaemia, compared with normoxia. Conversion to glutamine was slow, and concentrations increased later in hypoxia and ischaemia. For the determination of oxygen consumption from the model, TCA cycle flux was calculated as the product of the sum of fitted rates k_4 and k_5 and the sum of the tissue concentrations of glutamate, aspartate and TCA cycle intermediates. Multiplying the TCA_{flux} by 3 (a factor of 2 for the number of oxygen molecules used per turn of the cycle and a factor of 1.5 because approximately two-thirds of the substrates for oxidative phosphorylation are provided by the TCA cycle) gives MVO_2. Estimated and measured MVO_2 were closely correlated [MVO_{2Est}=–1.51+0.97×(MVO_{2Meas}), r=0.95], under ischaemic, hypoxic and normoxic conditions. In addition, k_4 and the mono-exponential clearance rate were closely correlated.

Sun et al. [54] simplified the six-tissue compartment model to a two-tissue compartment model (Fig. 5) by leaving out some compartments of the model of Ng et al. [32] Analysis time was limited to the first 5 (baseline, dipyridamole and dobutamine) to 10 (ischaemia and xylazine) minutes after tracer administration. This was done because the six-compartment model [32] is error sensitive and impractical. The compartments were left out because the conversion from glutamate to glutamine was found to be low and not present early after tracer administration. The concentration of labelled bicarbonate was rather constant, with an efflux rate much higher than production rate. Furthermore, concentrations in the pre-TCA cycle pool were very low with fast transit times. For determination of the TCA cycle flux, concentrations of glutamate, aspartate and TCA cycle intermediates were assumed to be identical in rat and dog hearts. The model was investigated in dogs under various conditions, including dipyridamole-induced hyperaemia and dobutamine infusion. Estimated and measured MVO_2 were closely correlated (MVO_{2Est}=0.033 + 0.690×$MVO_{2\ Meas}$, r=0.92). The underestimation of the MVO_{2Meas} by the model was explained by the different tissue concentrations of glutamate, aspartate and TCA cycle intermediates in rat and dog hearts.

This two-tissue compartment model was also investigated in humans, with comparison to invasively measured MVO_2 [42]. A correlation r=0.74 between estimated and measured MVO_2 was reported (MVO_{2Est}= –0.019 + 1.008×MVO_{2Meas}). However, recalculations with the data provided in the publication show a closer correlation (r=0.85) with a slightly different equation (MVO_{2Est}=–0.0025+0.996×MVO_{2Meas}). These stud-

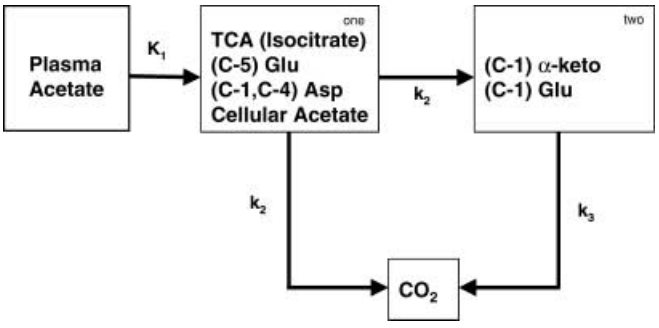

Fig. 5. Simplified two-tissue compartment model used by Sun et al. [42, 54]. The number of compartments was reduced because back-diffusion of the tracer was low and the transport of acetate into the TCA cycle was very fast. The glutamine pool was left out because of the low contribution to total activity early after administration of acetate. The bicarbonate pool was left out because the clearance of bicarbonate from the myocardium was high. Uptake into the cell is by rate K_1. Formation of CO_2 is at rates k_2 and k_3, which are said to be identical. Abbreviations as in Fig. 4

ies were only performed under resting conditions, and thus had a small range of MBF and MVO_2 values.

Van den Hoff et al. formulated a slightly different five-tissue compartment model (Fig. 6A) [55]. Based on the observations that rates of cellular uptake, back-diffusion, activation and uptake into the TCA cycle of labelled acetate, as well as wash-out rate of labelled CO_2, are substantially faster than the TCA cycle flux, two simplified models were defined (Figs. 6B and 3C). These models were evaluated with model prediction (computer simulation) based on data obtained in open-chest dogs by Armbrecht et al. [33] and in 41 patients. Simulations revealed a strong interaction between TCA cycle uptake and CO_2 washout rates, which was stabilised when CO_2 wash-out was fixed at 1 min^{-1}. Rates k_5 (0.03), k_6 (0.003) and k_7 (0.1) were responsible for the bi-exponential tissue clearance that was observed. When pool sizes were reconstructed in time, pool five (amino acids) contained approximately 100% of the tissue activity present after 30 min and was slowly clearing. The authors did not confirm these observations with analysis of biopsies of hearts, and they were not found by Ng et al. [32]. It was demonstrated that simplified two- and one-tissue compartment models would be sufficient for analysis of patient data. Data obtained in patients were corrected by a mean value for circulating activity and for blood volume of the tissue. Time-activity curves could be fitted well both with the simplified model and with a single-tissue compartment model. No results of linear regression analysis were reported. The data used as a basis for initial model parameters were obtained with a single gamma detector encompassing the LAD territory and were thus susceptible to noise and spillover from the blood pool. This may be at least one of the reasons for the high activity remaining in the curve after 40 min.

Additional observations

Influence of substrate availability

The influence of the availability of substrates on the clearance of acetate was studied by a number of authors [30, 33, 40, 41, 47, 48, 56, 57]. Buxton et al. observed no differences in ^{11}C-acetate clearance when lactate, hydroxybutyrate or palmitate was added to the perfusate [30]. Only when acetate was present in large non-tracer amounts in the perfusate, was TCA cycle flux underestimated [30]. The same group observed a slightly higher

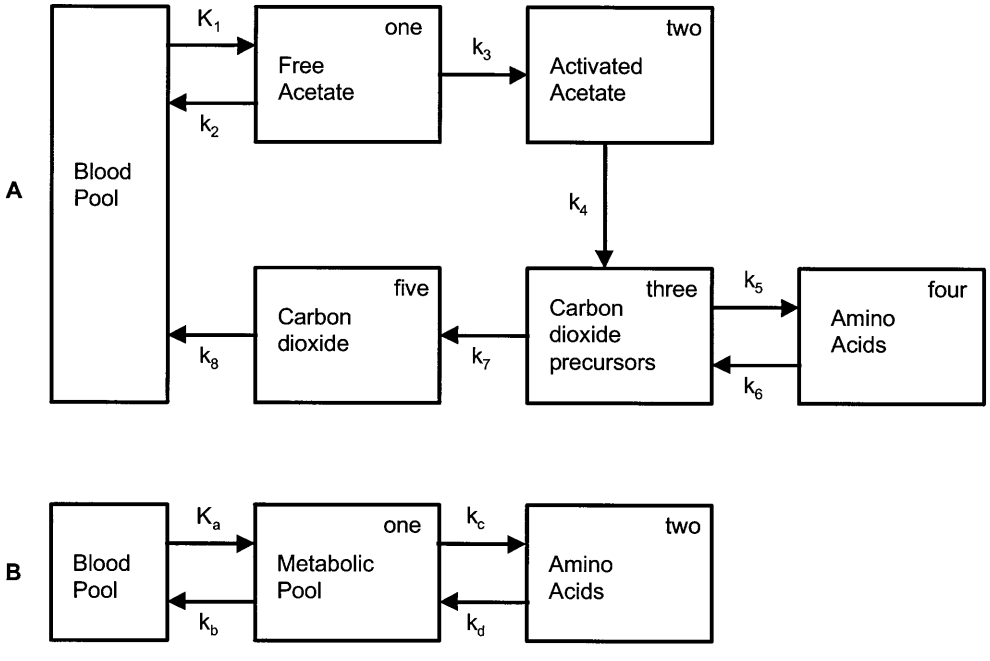

Fig. 6A, B. Models used by Van den Hoff et al. [55]. **A** Five-tissue compartment model, describing the metabolic fate of acetate. This model was used to generate tissue time-activity curves with the computer, based on data of Armbrecht et al. [33]. **B** Simplified model based on observations and computer simulations. Clearance is determined by k_b

k_1/MVO_2 ratio in dogs when predominantly carbohydrates were used as fuel for the heart [41]. No differences were found by Brown et al. after normalisation of clearance rates to MVO_2 [40]. Armbrecht et al. [48] observed a slight but significant decrease in k_{mono}/RPP in patients after an oral glucose load. Kotzerke et al. [56] observed a 15% higher clearance of acetate ($P<0.05$) in subjects studied with a euglycaemic-hyperinsulinaemic clamp with additional administration of intralipid (FFA source). The RPP was similar to that in the other patient groups in this study. Without the additional infusion of FFA, clearance rates of clamped subjects were not significantly different from normal. Tamaki et al. [47] and Hicks et al. [57] observed no differences in clearance rates after changing substrate availability.

Though some effects of substrate availability were found in these studies, they were small and could largely be explained by different workloads. The results of Kotzerke et al. [56] could be explained by the higher amount of oxygen needed to obtain the same amount of ATP when FFA is the substrate of myocardial metabolism. Also important is the influence of acetate present in non-tracer amounts [30]. As acetate is the end product of ethanol metabolism, it can be present in subjects who have ingested large amounts of ethanol-containing liquids in the hours prior to the study. Significant effects of ethanol ingestion on plasma acetate levels have been reported [58].

Regional variation of ^{11}C-acetate clearance

Clearance of ^{11}C-acetate has been found to be homogeneous in most studies that have looked for regional differences in normal myocardium [39, 46, 47, 48, 57]. One study observed a higher clearance in septal and anterior regions compared with lateral regions, as well as higher clearance rates in basal and midventricular regions compared with apical regions [56]. Another study observed lower septal clearance [41]. These variations were minor, however, ranging only from –7% to 7%.

Considerations of validation, modelling and additional observations

The results discussed above show that externally detected clearance of labelled acetate from the myocardium is closely related to labelled CO_2 production, measured MVO_2 and indices of MVO_2. Clearance is bi-exponential in animals and also in humans when workload is increased, but mono-exponential when workload is low, both in humans and in animals. Substrate availability did not have a significant influence on clearance when it was compared with measured MVO_2, indicating that metabolic standardisation is not necessary for determination of oxygen consumption. There was little to no regional variation.

Clearance rates determined with kinetic models were closely correlated with measured MVO_2. Exact determination of MVO_2 by modelling is only possible when concentrations of glutamate, aspartate and TCA cycle intermediates are known; these concentrations can vary between species, but also in diseases. Human studies using modelling were mostly done under resting conditions and results were not always related to measured MVO_2. This warrants further investigations with wider flow and MVO_2 ranges. Other investigations should be directed towards measurement of the blood content of the myocardium and the perfusable tissue to apply these values in future models.

Determination of myocardial blood flow with ^{11}C-acetate

Gropler et al. compared myocardial tissue activities after bolus injection of ^{11}C-acetate and ^{15}O-H_2O [59]. Activities were determined in a time frame of 60–180 s after injection of ^{11}C-acetate and in a time frame of 120 s after appearance in the left atrium of the ^{15}O-H_2O bolus. The image of ^{15}O-H_2O was corrected for intravascular activity with the use of ^{15}O-CO. Activities per segment were normalised to the segment with the highest activity. Twenty-two patients with CAD and wall motion abnormalities were studied. Fourteen patients had suffered at least one myocardial infarction. The relative uptake of acetate was closely correlated with relative MBF determined by ^{15}O-H_2O (acetate=0.75×(^{15}O-H_2O)+0.22, r=0.88). Correction for spillover of the ^{11}C-acetate image with the use of the ^{15}O-CO data for five patients revealed a correlation with a similar slope to the uncorrected data (r=0.90), but decreased the y-intercept of the regression line by 29%. Clearance and relative uptake of acetate were also correlated (r=0.66).

Chan et al. compared relative tracer concentrations (normalisation to segment with highest activity) of ^{11}C-acetate and of ^{13}N-ammonia [60]. In addition, net extraction of ^{11}C-acetate and ^{13}N-ammonia (obtained by dividing tissue concentration by an image-derived input integral) was compared. The 4th minute was chosen for acetate because clearance from myocardium is low until this time point. The 4th to 19th minutes were chosen for ammonia because no additional uptake is to be expected after 4 min and trapping of the tracer. Input was integrated for the first 4 min for acetate and for the first 2 min for ammonia. Fifteen patients with coronary artery disease were studied, of whom 14 had previous myocardial infarction. Eight segments were analysed per patient. Ammonia and acetate relative tissue concentrations were closely correlated (acetate=0.88 × ammonia + 0.079, r=0.94), as were ammonia and acetate net extraction (acetate=0.55 × ammonia + 0.08, r=0.87). The slopes were significantly different from one and the intercepts were not zero, which could be explained partially by the im-

mediate metabolism of acetate and the trapping of ammonia by the myocardium. This [60] and the former report [59] suggest that acetate could also be used to determine myocardial perfusion.

Krivokapich et al. used the Renkin-Crone equation reported by Armbrecht et al. [33] to determine MBF with ^{11}C-acetate in a model similar to that of ^{13}N-ammonia [45]. Subjects were studied at rest and during infusion of dobutamine. A close correlation was found between both tracers ($flow_{acetate}=1.1 \times flow_{ammonia} - 0.088$), $r=0.92$).

Sun et al. correlated K_1 of acetate with MBF determined with ammonia [42]. A close correlation was found [$K_1=0.15+0.73\times$(MBF); $r=0.93$], over an MBF range of 0.5–1.0 ml/min per gram. Further studies over a wider range of MBF are required to assess whether acetate could also be used to measure MBF.

Use of acetate in ischaemia and viability studies

After the initial validation studies of acetate to determine MVO_2 non-invasively, it was used in several experimental and clinical studies, most of them assessing ischaemia, stunning and hibernation. The majority of these studies used simple mono-exponential curve fitting procedures, although some applied models.

Acetate clearance in (post-)ischaemic myocardium in animals

Buxton et al. studied dogs 2 and 24 h after a 20-min occlusion of the LAD [61]. In post-ischaemic regions, clearance rates at 2 h were reduced to 69%±15% ($P<0.001$) of those in remote regions, recovering to 90%±17% at 24 h (not significantly different from baseline). There was a tendency for lower clearance rates in regions with more severe wall motion disturbances. Regions with increased fluorine-18 fluorodeoxyglucose (FDG) uptake at 24 h had significantly depressed acetate metabolism, whereas regions with normal or even decreased uptake of FDG had normal turnover of acetate. The increased FDG uptake may have been due to increased anaerobic metabolism in reperfused myocardium. The same group studied dogs serially over a 1-month period after a 3-h occlusion of the LAD [62]. At the time of occlusion, MBF (ammonia) was more depressed than acetate clearance (comparison with normal regions), suggesting enhanced oxygen extraction. After restoration of MBF, acetate clearance initially remained depressed, showing recovery in parallel with the slow recovery of function. FDG uptake was initially enhanced in post-ischaemic regions and normalised in time, again suggesting increased anaerobic metabolism early after reperfusion. Weinheimer et al. observed that preservation of ^{11}C-acetate clearance after 1 week and the recovery of wall motion after 4 weeks were significantly correlated in dogs after a 1- or 4-h occlusion of the LAD [63]. Similar observations were reported by Heyndrickx et al. after a 1-h occlusion of the circumflex artery in dogs [64].

In experiments in open-chest dogs with repeated occlusion of the LAD, a reduction of myocardial blood flow by 21% was observed 45 min after four ischaemic episodes of 5 min with intervals of 5 min, together with a decrease in systolic function of 90%. Ninety minutes after the ischaemic episodes, MVO_2 was unaltered compared with baseline, while systolic function was still depressed by 70% [65]. In observations up to 1 week after similar ischaemic bouts, blood flow was restored promptly while acetate clearance in ischaemic regions was significantly depressed and gradually recovered over the week, along with restoration of function and glucose consumption, measured with FDG [66]. These results indicate that recovery of function after coronary occlusion may be dependent on preservation of myocardial oxidative metabolism.

Bergmann et al. studied the effect of paired pacing (a method to increase inotropy [67, 68, 69], used initially to demonstrate viability) in canine myocardium stunned by a 15-min occlusion of the LAD [70]. One hour after reperfusion, acetate clearance of stunned segments was reduced to 71%±27% of that of normal regions, whereas MBF was near normal. Stunned segments showed improvement of wall motion with paired pacing, accompanied by recovery of acetate clearance to values comparable to those of normal regions. MBF in stunned areas showed an increase similar to the increase in flow in remote areas with pacing. Similar results, after 25 min occlusion of the LAD, were obtained by Hashimoto et al. with the use of dobutamine as an inotropic stimulus [71]. These studies indicate that enhancement of function in regions with stunned myocardium with appropriate stimuli is dependent on oxidative metabolism.

Acetate clearance in ischaemia in humans

In patients with transmural, complete myocardial infarction, clearance of ^{11}C-acetate was markedly diminished in peri-infarct and infarct regions (to 68% of normal in peri-infarct, 48% in infarct and 21% in central infarct regions) [72]. Neither acetate clearance rate nor function recovered after 7 days. In patients receiving reperfusion therapy for anterior myocardial infarction, ^{11}C-acetate clearance in the central area of myocardial infarction was reduced by 51% [73]. In contrast to the findings of Buxton et al. [61], acetate clearance was higher in regions with an MBF-FDG mismatch than in regions with an MBF-FDG match, indicating preserved oxidative metabolism in mismatch areas. Acetate clearance was positively and linearly correlated with MBF and independent of the MBF-FDG pattern. Similar results were obtained by Czernin et al. in 22 patients with recent myocardial infarction, ten of whom were treated with reperfusion

therapy [74]. Thus, oxidative metabolism was relatively preserved in areas with reduced MBF and a mismatch, indicating preserved oxidative metabolism and possibly an enhanced extraction fraction of oxygen.

A study in patients with acute myocardial infarction who were treated with thrombolysis or coronary angioplasty showed similar results [75]. Interestingly, patients using beta-blockade had a significantly reduced clearance rate in the remote area compared with patients not using beta-blockade, despite similar RPPs. In infarction areas, a similar, but not significant effect of beta-blockade on acetate clearance was present. This finding is an indication of the effect of beta-blockade on MVO_2.

Hicks et al. assessed both oxidative metabolism and perfusion with ^{11}C-acetate in patients with acute myocardial infarction [76]. The extent of myocardial perfusion abnormality was defined as the relative amplitude of the mono-exponential fit of the time-activity curve. Relatively preserved acetate clearance, as compared with perfusion, was associated with recovery of function. Absolute acetate clearance was not different between segments that showed improvement of function and those that were irreversibly dysfunctional, because of a considerable overlap between the two groups. In patients with myocardial infarction treated with intravenous thrombolysis, serial scanning with ^{11}C-acetate and ^{15}O-H_2O revealed immediate restoration of blood flow shortly after reperfusion therapy. Recovery of function was associated with gradual recovery of oxidative metabolism [77].

In patients with a coronary occlusion without signs of myocardial infarction, clearance of ^{11}C-acetate at rest was lower in segments with abnormal wall motion than in those with normal wall motion, which themselves showed similar clearance to that in remote segments [78]. The reduction of acetate clearance in segments with abnormal wall motion was accompanied by a reduction of perfusion reserve, whereas the segments with normal wall motion had a normal perfusion reserve. In patients with unstable angina pectoris, a proximal LAD stenosis and severe dysfunction of the anterior myocardium shortly after revascularisation (PTCA), normal MBF and near-normal oxygen consumption with ^{11}C-acetate were found, suggesting not only a perfusion-contraction mismatch but also a decreased myocardial efficiency in these segments [79]. Baseline flow was normal in both types of segment.

Janier et al. stimulated patients with an occluded coronary artery and normal myocardial wall motion with dobutamine and compared these patients with normal volunteers [80]. Metabolic reserve, defined as the percentage increase in clearance of ^{11}C-acetate under dobutamine stimulation, was identical in both groups. Perfusion reserve was limited in the areas supplied by the occluded coronary arteries compared with perfusion reserve in volunteers. This suggests an increased oxygen extraction fraction in the areas supplied by the stenotic coronary artery when dobutamine is used as a stimulus.

Ohte et al. studied the phenomenon of reverse redistribution on exercise redistribution–late redistribution thallium-201 scans [81]. Patients with this phenomenon were also studied with ^{11}C-acetate at rest. It was observed that regions with reverse redistribution had a lower clearance rate of ^{11}C-acetate than normal regions, but a higher clearance rate than segments with irreversible perfusion defects. This finding suggests that reverse redistribution on thallium scans is associated with viability.

Acetate clearance and recovery of function after revascularisation

Gropler et al. studied patients with LV dysfunction due to coronary artery disease with [82] and without [83] previous myocardial infarction prior to revascularisation. Dysfunctional but viable (recovery of function after revascularisation) segments exhibited relatively preserved ^{11}C-acetate clearance (74% and 95% of clearance in normal regions in patients with and without infarct, respectively), whereas non-viable segments showed reduced metabolism (45% and 66% of clearance in normal regions, respectively). This finding suggests that recovery of function after revascularisation is dependent on maintenance of oxidative metabolism. ^{18}F-FDG uptake (activity at 45 min normalised to maximum activity) was variable in these patients, particularly in the non-viable group. Some of the patients were restudied after revascularisation. Metabolism of ^{11}C-acetate showed improvement in viable segments only, as did FDG uptake, despite restoration of MBF to all segments.

Conversano et al. studied 17 patients with chronically reduced left ventricular function due to coronary artery disease before revascularisation [84]. MBF (^{15}O-H_2O), acetate clearance and FDG metabolism were measured. Irreversible dysfunctional segments exhibited a lower acetate clearance than reversible dysfunctional segments. Acetate clearance in segments with reversible dysfunction and normal MBF (^{15}O-H_2O) was not different from that in normal segments. Clearance was significantly reduced in reversible segments with a reduced MBF but was significantly higher than in segments that were irreversibly damaged. FDG uptake (related to flow) was higher in reversible segments with a low MBF and in irreversible segments than in reversible segments with a normal MBF. Thus, acetate clearance could be used to distinguish between viable and non-viable myocardium, especially in segments with enhanced FDG uptake and reduced MBF.

Hata et al. used low-dose dobutamine infusion to determine viability in regions with old myocardial infarction [85]. Baseline clearance rates were higher in viable (recovery of function after revascularisation) than in non-viable segments but a considerable overlap was present. Dobutamine increased mono-exponential clear-

Table 4. Comparison of studies predicting viability based on acetate clearance

Author	Modality	Compared to:	No. of segments	Sens.	Spec.	PPV	NPV
Gropler et al. [86]	Oxidative metabolism (acetate)	Recovery of function	116	87 (40/46)	71 (50/70)	67 (40/60)	89 (50/56)
	FDG uptake	Recovery of function	116	83 (38/46)	50 (35/70)	52 (38/73)	81 (35/43)
Rubin et al. [87]	Oxidative metabolism (acetate)	Recovery of function	54	78 (25/32)	86 (19/22)	89 (25/28)	73 (19/26)
	FDG uptake	Recovery of function	54	81 (26/32)	36 (8/22)	65 (26/40)	57 (8/14)
Lee et al. [88]	Oxidative metabolism (acetate)	Dobutamine echocardiography	145	84 (47/56)	38 (34/89)	46 (47/102)	79 (34/43)
Wolpers et al. [89]	Oxidative metabolism (acetate)	Recovery of function	114	77 (46/60)	48 (26/54)	62 (46/74)	65 (26/40)
	MBF (acetate)	Recovery of function	114	93 (56/60)	67 (36/54)	76 (56/74)	90 (36/40)
	FDG uptake >50% of max.	Recovery of function	114	88 (53/60)	74 (40/54)	78 (53/67)	85 (40/47)
Combined	Oxidative metabolism (acetate)	Recovery of function	284	80 (111/138)	65 (95/146)	69 (111/162)	78 (95/122)
Combined	FDG uptake	Recovery of function	284	85 (117/138)	57 (83/146)	65 (117/180)	80 (83/104)
Combined	Oxidative metabolism (acetate)	Mixed	429	81 (158/194)	55 (129/235)	60 (158/264)	78 (129/165)

Sens., Sensitivity; Spec., specificity; PPV, positive predictive value; NPV, negative predictive value

ance of acetate in viable segments but not in non-viable segments. After normalisation of clearance rates to segments with normal wall motion, clearance increased from 71%±16% to 83%±10% in viable segments, whereas it decreased from 43%±13% to 27%±10% in non-viable segments, thus helping to distinguish between viable and non-viable myocardium. Similar results were obtained for normalised uptake of acetate, indicating that this may be used as a predictor of recovery of function as well. Thus, these findings indicate that changes in acetate clearance with low-dose dobutamine infusion may help to distinguish viable myocardium from non-viable myocardium.

Prediction of recovery of function by acetate clearance

The studies mentioned previously [63, 64, 70, 71, 82, 83, 84, 85] led to investigations to predict recovery of function after revascularisation based on acetate clearance. A summary of these studies is given in Table 4.

Gropler et al. studied 34 patients with and without previous myocardial infarction prior to revascularisation [86]. Clearance of acetate and FDG uptake were determined, as well as myocardial perfusion (based on the early uptake of acetate). Of 116 dysfunctional segments, 70 were classified as non-viable and 46 as viable (recovery of function after revascularisation). Threshold criteria for clearance of acetate and FDG uptake were formulated based on absolute values obtained in normal volunteers. Receiver operating characteristic curves showed that absolute acetate clearance and absolute FDG uptake were the best predictors for recovery of function. Based on the thresholds, 67% of the segments were correctly judged as viable and 89% as non-viable using ^{11}C-acetate, whereas ^{18}F-FDG uptake correctly judged 52% as viable and 81% as non-viable.

Patients who suffered from acute myocardial infarction were studied prior to revascularisation by Rubin et al. [87] Perfusion was determined by early uptake of acetate and metabolism by acetate clearance and FDG up-

take. Values were normalised to the area with the highest uptake for each tracer. Thresholds came from a database with normal volunteers. Of 54 dysfunctional segments on echocardiography, 32 were reversibly dysfunctional and were thus viable. Clearance of acetate predicted 89% correctly to be viable, whereas FDG predicted only 65% correctly. Of the 22 non-viable segments, 73% were correctly predicted by acetate and only 57% by FDG.

Lee et al. studied the presence of contractile reserve (assessed with dobutamine echocardiography) in relation to change in acetate clearance and MBF (^{15}O-H_2O) [88]. Although lower than in normal segments, acetate clearance and MBF were higher in myocardial segments with contractile reserve than in segments having no such reserve. The two categories showed a considerable overlap, however. The pattern under dobutamine stimulation was similar. Viability determined from resting acetate clearance (cut-off values ranging from 0.051 min^{-1} in apical segments to 0.056 min^{-1} in inferior segments) had a sensitivity of 84% and a specificity of 38%. These percentages were lower than previously reported.

Wolpers et al. also determined threshold values for viability [89]. In contrast to other studies mentioned here, absolute MBF, derived from modelled acetate uptake rate and the Renkin-Crone equation from Armbrecht [33], was the best predictor of viability. Absolute acetate clearance (also derived from the model) was a worse predictor than increase in glucose metabolism of 50% or more (derived from Patlak analysis and normalised to normal segments) or a normalised MBF-normalised FDG mismatch of more than 16%.

In Table 4, estimates of sensitivity, specificity and positive and negative predictive values are also given when these studies are combined. For acetate versus recovery of function, lumped sensitivity is 80% and lumped specificity 65%, with positive and negative predictive values of 69% and 78%, respectively. Compared with FDG uptake, these values are in a similar range: sensitivity is slightly lower but specificity is higher, while predictive values are virtually identical. When dobutamine echocardiography is included as a detector of viability, sensitivity remains the same while specificity drops, as does the positive predictive value. This indicates overestimation of viability when using acetate clearance as a predictor of viability. The studies all used absolute cut-off values of acetate clearance for predicting recovery of function. This may be incorrect, because MVO_2 and thus clearance of acetate from the myocardium is dependent on cardiac work. None of these studies used acetate clearance rates relative to normal functioning myocardium (on echocardiographic examination and thus viable) to predict recovery of function, or clearance rates normalised to workload. Further research using normalised criteria needs to be performed.

Acetate as a tracer of MVO_2 in conditions other than coronary artery disease

Aortic valve disease

Acetate clearance in patients with aortic stenosis and regurgitation was determined by Hicks et al. [90]. Absolute acetate clearance was significantly higher in patients with aortic valve disease than in normal volunteers, but this was accompanied by a higher index of cardiac work. The *k*/RPP ratio (corrected for the gradient over the aortic valve) in patients with aortic stenosis was lower, suggesting a lower MVO_2 for a given work rate. The clearance rate and the gradient-corrected RPP were linearly correlated in patients with aortic stenosis, but not in patients with regurgitation. This finding could be due to increased stroke work (volume load) in patients with aortic regurgitation compared to patients with aortic stenosis. Acetate clearance was only slightly heterogeneous throughout the left ventricle. In another study, oxidative metabolism of the free wall of the right ventricle was determined in patients with aortic stenosis: acetate clearance was linearly correlated with the RPP of this ventricle [91].

Hypertrophic cardiomyopathy

Tadamura et al. demonstrated reduced clearance of acetate in hypertrophied compared to non-hypertrophied segments in patients with hypertrophic non-obstructive cardiomyopathy [92]. Clearance in non-hypertrophied segments was similar to that in normal volunteers. MBF (derived from peak activity of acetate) in hypertrophied and non-hypertrophied segments was not different, but the reduction in metabolic rate of glucose was similar to that in acetate clearance. No differences were found between asymptomatic and symptomatic patients. In the same type of patient, similar results were reported by Ishiwata et al. [93, 94]. Regional work rate (RWR) was significantly decreased in hypertrophied regions compared with non-hypertrophied regions, but also in non-hypertrophied regions when compared with normal volunteers. Clearance rate divided by RWR (*k*/RWR) was remarkably higher in hypertrophied regions, indicating a decreased efficiency in hypertrophic regions [93].

Dilated cardiomyopathy

Beanlands et al. investigated myocardial efficiency in patients with dilated (non-ischaemic) cardiomyopathy with dobutamine and nitroprusside [95, 96]. Acetate clearance was derived by modelling and converted to MVO_2 after validation in these patients with actually measured MVO_2. Myocardial efficiency (work divided by MVO_2) improved with the administration of dobu-

tamine, despite an increase in MVO_2 [95]. Administration of nitroprusside decreased MVO_2 and increased efficiency [96]. Another study determined the relation between regional function and oxidative metabolism under resting conditions in a similar population [97]. Multivariate regression analysis showed a direct relationship between increased function and acetate clearance (P=0.02). Concordance between function and acetate clearance was 0.87 (95% confidence interval 0.70–1.0). Another study also showed reduced myocardial efficiency in patients with idiopathic dilated cardiomyopathy [98]. Myocardial efficiency showed a strong, positive correlation with ejection fraction.

Other studies

Torizuka et al. studied hyperthyroid patients before and after treatment with propanolol [99]. Myocardial acetate clearance rates, both absolute and relative to the RPP, were higher in untreated patients than in normal volunteers. Clearance rate and RPP were not strongly correlated in patients, however. After 2 weeks of treatment the RPP normalised to values found in volunteers, but clearance remained higher, as did k/RPP. This finding suggests a lower efficiency in patients with hyperthyroidism, which might be associated with the higher contractility or with oxygen wasting.

Hattori et al. studied patients with non-insulin-dependent diabetes mellitus (NIDDM) at rest and with dobutamine [100]. Patients showed a more heterogeneous metabolism of ^{11}C-acetate than did healthy volunteers. The acetate clearance and RPP were not significantly correlated in patients, whereas they were in volunteers (r=0.31 vs r=0.89). This may have been due to the altered substrate availability in diabetic patients, with a significant effect on the work-MVO_2 relationship. As discussed earlier in this review, substrate availability may have a significant influence on the work-oxygen consumption relationship. These data suggest that although substrate availability had little influence on acetate metabolism in previous studies, patients with diabetes mellitus may not have the same oxidative metabolism as other patient groups. It is important to emphasise that in Hattori et al.'s study, k_{mono} was correlated to the RPP and not to measured MVO_2. This could have had a significant influence, because patients with NIDDM often have a disturbed fatty acid metabolism. FFAs in plasma are also increased by dobutamine. When correlating to the RPP, one can misjudge the relationship between acetate clearance and MVO_2 because of the number of ATP produced per molecule of oxygen consumed, as explained in "Rationale of using labelled acetate as a tracer of MVO_2" previously in this review.

Hutchins et al. studied the effect of denervation of canine myocardium on MBF (^{13}N-ammonia) and oxidative metabolism (acetate clearance) [101]. An area in the LAD territory was denervated by the epicardial application of phenol in five dogs. Five dogs served as controls after a sham operation. A reduction of innervation (^{11}C-hydroxyephedrine) with a reduction in oxidative metabolism was found without a reduction in MBF. The authors hypothesised that the reduced oxidative metabolism was due to the reduced contractility regulation caused by the denervation of the region.

Bengel et al. studied patients who had undergone orthotopic heart transplantation [102]. Clearance of ^{11}C-acetate was similar to that in volunteers and showed no regional differences, with similar RPPs. This finding does not confirm the finding of Hutchins et al. [101], and the authors speculate on partial re-innervation of the transplanted heart, although cardiac innervation was not determined. The report by Bengel et al. [102] is also not in agreement with a report by Rechavia et al. [103], in which an increased cardiac FDG metabolism disproportionate to MBF was found in cardiac transplant patients. Rechavia et al. [103] speculated on decreased myocardial efficiency after heart transplantation; however, Bengel et al. [102] hypothesise that there is a transition of substrate usage towards glucose in these patients but that TCA cycle flux and thus oxygen usage is not altered.

General considerations

Overall myocardial oxidative metabolism can be assessed non-invasively by PET with ^{11}C-acetate as a tracer, both on a global and on a regional basis. It has been demonstrated that the kinetics of ^{11}C-acetate reflect TCA cycle flux and thereby MVO_2 under a wide range of haemodynamic conditions in animals and humans. Clearance rates from mono- and bi-exponential curve-fitting procedures as well as from model fitting have been found to correlate closely with measured MVO_2. Some studies have used values obtained from mono-exponential curve-fitting procedures to calculate MVO_2, while others have used values from model-fitted curves. Only a few studies have actually validated this with measured MVO_2. One of the problems is the unknown concentration of glutamate, aspartate and TCA cycle intermediates in the human heart, which may vary in diseases and ischaemia. Uptake and clearance of ^{11}C-acetate have been found to be independent of substrate utilisation by the heart, making this tracer preferable over substrate-dependent tracers. One of the major advantages of using PET is the ability to assess MVO_2 on a regional basis and the less invasive nature of the technique.

Another potential advantage of ^{11}C-acetate is the possibility of measuring MBF and MVO_2 simultaneously. Several studies have suggested that ^{11}C-acetate is as accurate in estimating MBF as other, already established flow tracers. This ability to combine flow-metabolism studies with the use of a single tracer is of great importance in the investigation of myocardial ischaemia and

coronary artery disease. Furthermore, ^{11}C-acetate has the potential to allow in vivo characterisation of the mechanisms responsible for the mechanical dysfunction in various cardiac diseases.

Based on the findings in validation studies, determination of oxidative metabolism by ^{11}C-acetate has been applied extensively in basic and clinical research. Virtually none of these studies have tried to actually measure MVO_2, and almost all of them have used simple monoexponential curve-fitting procedures. Nevertheless, our understanding of cardiac oxidative metabolism has grown, especially in coronary artery disease. It has become clear that preservation of myocardial oxidative metabolism is a prerequisite for recovery of function, both after myocardial infarction and in left ventricular dysfunction without infarction. Based on these findings, prediction of recovery of function after revascularisation has been attempted. Although considerable overlap with normal myocardium is present, clearance of acetate has been found to be just as adequate a predictor as ^{18}F-FDG uptake. Dobutamine may help to distinguish between viable and non-viable myocardium, as in echocardiography studies.

Other interesting findings are altered oxidative metabolism in patients with aortic stenosis, an increase in myocardial efficiency in patients with dilated cardiomyopathy after administration of dobutamine or nitroprusside and the decreased efficiency in patients with hypertrophic cardiomyopathy.

Because ^{11}C-acetate metabolism is theoretically not substrate dependent, it can be used in all types of patients, although one study suggests that in patients with diabetes, acetate metabolism is altered. However, when relating MVO_2 to indices of oxygen consumption, substrate availability may play an important role.

Additional work still needs to be done to validate models in humans under various workloads and myocardial blood flows, as well as in various diseases, in order to allow investigations of the effect and efficacy of therapies designed to improve myocardial function by reducing MVO_2. Furthermore, consensus needs to be reached on the best method for analysing ^{11}C-acetate studies. Further work is required to assess whether simple exponential fitting of clearance curves is sufficient for routine clinical studies. Future clinical investigations should explore the use of ^{11}C-acetate in patients with valvular disease. Previous investigations suggest that changes in MVO_2 relative to workload in patients with aortic stenosis are reversible after valve replacement, especially in those without dysfunction. In other words, changes in MVO_2 may be present in these patients before other signs or symptoms are present. Furthermore, MVO_2 has to be delineated in patients with left ventricular hypertrophy due to hypertension. Validation of measurements should be performed in these types of patients, using ^{15}O-H_2O for flow and ^{15}O-O_2 for oxygen extraction. The predictive value of ^{11}C-acetate for recovery of function has to be confirmed, not only when oxidative metabolism is compared with values obtained in normal volunteers but also when the patient is used as his own reference.

References

1. Camici P, Marraccini P, Marzilli M, Lorenzoni R, Buzzigoli G, Puntoni R, Boni C, Bellina CR, Klassen GA, L'Abbate A. Coronary hemodynamics and myocardial metabolism during and after pacing stress in normal humans. *Am J Physiol* 1989; 257:E309–E317.
2. Holmberg S, Varnauskas E. Coronary circulation during pacing-induced tachycardia. *Acta Med Scand* 1971; 190:481–490.
3. Holmberg S, Serzysko W, Varnauskas E. Coronary circulation during heavy exercise in control subjects and patients with coronary heart disease. *Acta Med Scand* 1971; 190:465–480.
4. Messer JV, Wagman RJ, Levine HJ, Neill WA, Krasnow N, Gorlin R. Patterns of human myocardial oxygen extraction during rest and exercise. *J Clin Invest* 1962; 41:725–742.
5. Bing RJ, Hammond MM, Handelsman JC, Powers SR, Spencer FC, Eckenhof JE, Goodale WT, Hafkenschiel JH, Kety SS. The measurement of coronary blood flow, oxygen consumption, and efficiency of the left ventricle in man. *Am Heart J* 1949; 38:1–24.
6. Leight L, DeFazio V, Talmers FN, Regan TJ, Hellems HK. Coronary blood flow, myocardial oxygen consumption and myocardial metabolism in normal and hyperthyroid human subjects. *Circulation* 1956; 14:90–99.
7. Brachfeld N, Bozer J, Gorlin R. Action of nitroglycerin on the coronary circulation in normal and mild cardiac subjects. *Circulation* 1959; 19:697–704.
8. Braunwald E. Control of myocardial oxygen consumption: physiologic and clinical considerations. *Am J Cardiol* 1971; 27:416–432.
9. McKeever WP, Gregg DE, Canney PC. Oxygen uptake of the nonworking left ventricle. *Circ Res* 1958; 6:612–623.
10. Klocke FJ, Braunwald E, Ross J Jr. Oxygen cost of electrical activation of the heart. *Circ Res* 1966; 18:357–365.
11. Fick A. Über die Messung den Blutquantums in der Herzventrikeln. *Sitzungb Phys Med Ges Würzburg* 1870;16.
12. Hoff HE, Scott HJ. Physiology (continued). *N Engl J Med* 1948; 239:120–126.
13. Klein O. Zur Bestimmung des zirkulatorischen Minutenvolumens beim Menschen nach dem Fickschen Prinzip. *Munchener Medizinische Wochenshrift* 1930; 77:1311–1312.
14. Nelson RR, Gobel FL, Jorgensen CR, Wang K, Wang Y, Taylor HL. Hemodynamic predictors of myocardial oxygen consumption during static and dynamic exercise. *Circulation* 1974; 50:1179–1189.
15. Robinson BF. Relation of heart rate and systolic blood pressure to the onset of pain in angina pectoris. *Circulation* 1967; 35:1073–1083.
16. Sarnof SJ, Braunwald E, Welch GH, Case RB, Stainsby WN, Macruz R. Hemodynamic determinants of oxygen consumption of the heart with special reference to the tension time index. *Am J Physiol* 1958; 192:148–156.
17. Rooke GA, Feigl EO. Work as a correlate of canine left ventricular oxygen consumption, and the problem of catecholamine oxygen wasting. *Circ Res* 1982; 50:273–286.
18. Sonnenblick EH, Ross JJ, Covell JW, Kaiser GA, Braunwald E. Velocity of contraction as a determinant of myocardial oxygen consumption. *Am J Physiol* 1965; 209:919–927.

19. Strauer BE, Beer K, Heitlinger K, Hofling B. Left ventricular systolic wall stress as a primary determinant of myocardial oxygen consumption: comparative studies in patients with normal left ventricular function, with pressure and volume overload and with coronary heart disease. *Basic Res Cardiol* 1977; 72:306–313.
20. Baller D, Bretschneider HJ, Hellige G. Validity of myocardial oxygen consumption parameters. *Clin Cardiol* 1979; 2:317–327.
21. Suga H, Hayashi T, Shirahata M, Suehiro S, Hisano R. Regression of cardiac oxygen consumption on ventricular pressure-volume area in dog. *Am J Physiol* 1981; 240:H320–H325.
22. Baller D, Bretschneider HJ, Hellige G. A critical look at currently used indirect indices of myocardial oxygen consumption. *Basic Res Cardiol* 1981; 76:163–181.
23. Baller D, Schenk H, Strauer BE, Hellige G. Comparison of myocardial oxygen consumption indices in man. *Clin Cardiol* 1980; 3:116–122.
24. Suga H, Yasumura Y, Nozawa T, Futaki S, Igarashi Y, Goto Y. Prospective prediction of O_2 consumption from pressure-volume area in dog hearts. *Am J Physiol* 1987; 252:H1258–H1264.
25. Iida H, Rhodes CG, Araujo LI, Yamamoto Y, De Silva R, Maseri A, Jones T. Noninvasive quantification of regional myocardial metabolic rate for oxygen by use of $^{15}O_2$ inhalation and positron emission tomography. Theory, error analysis, and application in humans. *Circulation* 1996; 94: 792–807.
26. Yamamoto Y, De Silva R, Rhodes CG, Iida H, Lammertsma AA, Jones T, Maseri A. Noninvasive quantification of regional myocardial metabolic rate of oxygen by $^{15}O_2$ inhalation and positron emission tomography. Experimental validation. *Circulation* 1996; 94:808–816.
27. Bol A, Iida A, Essamri B, Vanbutsele R, Labar D, Grandin C, Wijns W, Melin J. A. Assessment of myocardial oxidative reserve with PET: comparison of C-11 acetate kinetics with quantitation of metabolic rate of oxygen (MRO_2) using O-15 O_2. *J Nucl Med* 1991; 32:988–989.
28. Opie LH. *The heart. Physiology, from cell to circulation. 3rd edn.* Philadelphia New York: Lipincott-Raven, 1997.
29. Beinert H, Green DE, Hele P, Hift H, Von Korff RW, Ramakrishnan CV. The acetate activating enzyme system of heart muscle. *J Biol Chem* 1953; 203:35–45.
30. Buxton DB, Schwaiger M, Nguyen A, Phelps ME, Schelbert HR. Radiolabeled acetate as a tracer of myocardial tricarboxylic acid cycle flux. *Circ Res* 1988; 63:628–634.
31. Randle PJ, England PJ, Denton RM. Control of the tricarboxylate cycle and its interactions with glycolysis during acetate utilization in rat heart. *Biochem J* 1970; 117:677–695.
32. Ng CK, Huang S-C, Schelbert HR, Buxton DB. Validation of a model for [1-^{11}C]acetate as a tracer of cardiac oxidative metabolism. *Am J Physiol* 1994; 266:H1304–H1315.
33. Armbrecht JJ, Buxton DB, Schelbert HR. Validation of [1-^{11}C]acetate as a tracer for noninvasive assessment of oxidative metabolism with positron emission tomography in normal, ischemic, postischemic, and hyperemic canine myocardium. *Circulation* 1990; 81:1594–1605.
34. Allan RM, Selwyn AP, Pike VW, Eakins MN, Maseri A. In vivo experimental and clinical studies of normal and ischemic myocardium using ^{11}C-acetate. *Circulation* 1980; 62:III-74.
35. Selwyn AP, Allan RM, Pike VW, Fox K, Maseri A. Positive labeling of ischemic myocardium: a new approach in patients with coronary artery disease. *Am J Cardiol* 1981; 47:481.
36. Allan RM, Pike VW, Maseri A, Selwyn AP. Myocardial metabolism of ^{11}C-acetate: experimental and patient studies. *Circulation* 1981; 64:IV-75.
37. Pike VW, Eakins MN, Allan RM, Selwyn AP. Preparation of [1-^{11}C]acetate – an agent for the study of myocardial metabolism by positron emission tomography. *Int J Appl Radiat Isot* 1982; 33:505–512.
38. Brown M, Marshall DR, Sobel BE, Bergmann SR. Delineation of myocardial oxygen utilization with carbon-11-labeled acetate. *Circulation* 1987; 76:687–696.
39. Brown MA, Myears DW, Bergmann SR. Noninvasive assessment of canine myocardial oxidative metabolism with carbon-11 acetate and positron emission tomography. *J Am Coll Cardiol* 1988; 12:1054–1063.
40. Brown MA, Myears DW, Bergmann SR. Validity of estimates of myocardial oxidative metabolism with carbon-11 acetate and positron emission tomography despite altered patterns of substrate utilization. *J Nucl Med* 1989; 30:187–193.
41. Buxton DB, Nienaber CA, Luxen A, Ratib O, Hansen H, Phelps ME, Schelbert HR. Noninvasive quantitation of regional myocardial oxygen consumption in vivo with [1-^{11}C]acetate and dynamic positron emission tomography. *Circulation* 1989; 79 :134–142.
42. Sun KT, Yeatman A, Buxton DB, Chen K, Johnson JA, Huang S-C, Kofoed KF, Weismueller S, Czernin J, Phelps M, Schelbert HR. Simultaneous measurement of myocardial oxygen consumption and blood flow using [1-carbon-11]acetate. *J Nucl Med* 1998; 39:272–280.
43. Schulz R, Kappeler C, Coenen H, Bockisch A, Heusch G. Positron emission tomography analysis of [1-(11)C] acetate kinetics in short-term hibernating myocardium. *Circulation* 1998; 97:1009–1016.
44. Henes CG, Bergmann SR, Walsh MN, Sobel BE, Geltman EM. Assessment of myocardial oxidative metabolic reserve with positron emission tomography and carbon-11 acetate. *J Nucl Med* 1989; 30:1489–1499.
45. Krivokapich J, Huang S-C, Schelbert HR. Assessment of the effects of dobutamine on myocardial blood flow and oxidative metabolism in normal human subjects using nitrogen-13 ammonia and carbon-11 acetate. *Am J Cardiol* 1993; 71:1351–1356.
46. Tamaki N, Magata Y, Takahashi N, Kawamoto M, Torizuka T, Yonekura Y, Tadamura E, Okuda K, Ono S, Nohara R. Oxidative metabolism in the myocardium in normal subjects during dobutamine infusion. *Eur J Nucl Med* 1993; 20:231–237.
47. Tamaki N, Magata Y, Takahashi N, Kawamoto M, Torizuka T, Yonekura Y, Nishizawa S, Sadato N, Tadamura E, Ono S, Nohara R, Kambara H, Konishi J. Myocardial oxidative metabolism in normal subjects in fasting, glucose loading and dobutamine infusion states. *Ann Nucl Med* 1992; 6:221–228.
48. Armbrecht JJ, Buxton DB, Brunken RC, Phelps ME, Schelbert HR. Regional myocardial oxygen consumption determined noninvasively in humans with [1-^{11}C]acetate and dynamic positron tomography. *Circulation* 1989; 80:863–872.
49. Vanoverschelde J-LJ, Wijns W, Essamri B, Bol A, Robert A, Labar D, Cogneau M, Michel C, Melin JA. Hemodynamic and mechanical determinants of myocardial O_2 consumption in normal human heart: effects of dobutamine. *Am J Physiol* 1993; 265:H1884–H1892.
50. Porenta G, Cherry S, Czernin J, Brunken R, Kuhle W, Hashimoto T, Schelbert HR. Noninvasive determination of myocardial blood flow, oxygen consumption and efficiency in

normal humans by carbon-11 acetate positron emission tomography imaging. *Eur J Nucl Med* 1999; 26:1465–1474.
51. Buck A, Wolpers HG, Hutchins GD, Savas V, Mangner TJ, Nguyen N, Schwaiger M. Effect of carbon-11-acetate recirculation on estimates of myocardial oxygen consumption by PET. *J Nucl Med* 1991; 32:1950–1957.
52. Raylman RR, Hutchins GD, Beanlands RS, Schwaiger M. Modeling of carbon-11-acetate kinetics by simultaneously fitting data from multiple ROIs coupled by common parameters. *J Nucl Med* 1994; 35:1286–1291.
53. Wolpers HG, Buck A, Nguyen N, Marcowitz PA, Armstrong WF, Starling MR, Hicks R, Mangner TJ, Schwaiger M. An approach to ventricular efficiency by use of carbon 11-labeled acetate and positron emission tomography. *J Nucl Cardiol* 1994; 1:262–269.
54. Sun KT, Chen K, Huang S-C, Buxton DB, Hansen HW, Kim AS, Siegel S, Choi Y, Müller P, Phelps ME, Schelbert HR. Compartment model for measuring myocardial oxygen consumption using [1-^{11}C] acetate. *J Nucl Med* 1997; 38:459–466.
55. van den Hoff J, Burchert W, Wolpers HG, Meyer G-J, Hundeshagen H. A kinetic model for cardiac PET with [1-carbon-11]-acetate. *J Nucl Med* 1996; 37:521–529.
56. Kotzerke J, Hicks RJ, Wolfe E, Herman WH, Molina E, Kuhl DE, Schwaiger M. Three-dimensional assessment of myocardial oxidative metabolism: a new approach for regional determination of PET-derived carbon-11-acetate kinetics. *J Nucl Med* 1990; 31:1876–1883.
57. Hicks RJ, Herman WH, Kalff V, Molina E, Wolfe ER, Hutchins G, Schwaiger M. Quantitative evaluation of regional substrate metabolism in the human heart by positron emission tomography. *J Am Coll Cardiol* 1991; 18:101–111.
58. Lindeneg O, Mellemgaard K, Lundquist F. Myocardial utilization of acetate, lactate and free fatty acids after ingestion of ethanol. *Clin Sci* 1964; 27:427–435.
59. Gropler RJ, Siegel BA, Geltman EM. Myocardial uptake of carbon-11-acetate as an indirect estimate of regional myocardial blood flow. *J Nucl Med* 1991; 32:245–251.
60. Chan SY, Brunken RC, Phelps ME, Schelbert HR. Use of the metabolic tracer carbon-11-acetate for evaluation of regional myocardial perfusion. *J Nucl Med* 1991; 32:665–672.
61. Buxton DB, Schwaiger M, Vaghaiwalla Mody F, Krivokapich J, Nienaber CA, Armbrecht JJ, Luxen A, Ratib O, Phelps ME, Schelbert HR. Regional abnormality of oxygen consumption in reperfused myocardium assessed with [1-^{11}C] acetate and positron emission tomography. *Am J Card Imaging* 1989; 3:276–287.
62. Buxton DB, Mody FV, Krivokapich J, Phelps ME, Schelbert HR. Quantitative assessment of prolonged metabolic abnormalities in reperfused canine myocardium. *Circulation* 1992; 85:1842–1856.
63. Weinheimer CJ, Brown MA, Nohara R, Perez JE, Bergmann SR. Functional recovery after reperfusion is predicated on recovery of myocardial oxidative metabolism. *Am Heart J* 1993; 125:939–949.
64. Heyndrickx GR, Wijns W, Vogelaers D, Degrieck Y, Bol A, Vandeplassche G, Melin JA. Recovery of regional contractile function and oxidative metabolism in stunned myocardium induced by 1-hour circumflex coronary artery stenosis in chronically instrumented dogs. *Circ Res* 1993; 72:901–913.
65. Kofoed KF, Hansen PR, Holm S, Hove JD, Chen K, Jin W, Jensen M, Iida H, Hesse B, Svendsen JH, Kelbaek H. Regional myocardial oxygen consumption estimated by carbon-11 acetate and positron emission tomography before and after repetitive ischemia. *J Nucl Cardiol* 2000; 7:228–234.
66. Di Carli MF, Prcevski P, Singh TP, Janisse J, Ager J, Muzik O, Vander HR. Myocardial blood flow, function, and metabolism in repetitive stunning. *J Nucl Med* 2000; 41:1227–1234.
67. Dyke SH, Cohn PF, Gorlin R, Sonnenblick EH. Detection of residual myocardial function in coronary artery disease using post-extra systolic potentiation. *Circulation* 1974; 50:694–699.
68. Nesto RW, Cohn LH, Collins JJJ, Wynne J, Holman L, Cohn PF. Inotropic contractile reserve: a useful predictor of increased 5 year survival and improved postoperative left ventricular function in patients with coronary artery disease and reduced ejection fraction. *Am J Cardiol* 1982; 50:39–44.
69. Becker LC, Levine JH, DiPaula AF, Guarnieri T, Aversano T. Reversal of dysfunction in postischemic stunned myocardium by epinephrine and postextrasystolic potentiation. *J Am Coll Cardiol* 1986; 7:580–589.
70. Bergmann SR, Weinheimer CJ, Brown MA, Perez JE. Enhancement of regional myocardial efficiency and persistence of perfusion, oxidative, and functional reserve with paired pacing of stunned myocardium. *Circulation* 1994; 89:2290–2296.
71. Hashimoto T, Buxton DB, Krivokapich J, Hansen HW, Phelps ME, Schelbert HR. Responses of blood flow, oxygen consumption, and contractile function to inotropic stimulation in stunned canine myocardium. *Am Heart J* 1994; 127:1250–1262.
72. Walsh MN, Geltman EM, Brown MA, Henes CG, Weinheimer CJ, Sobel BE, Bergmann SR. Noninvasive estimation of regional myocardial oxygen consumption by positron emission tomography with carbon-11 acetate in patients with myocardial infarction. *J Nucl Med* 1989; 30:1798–1808.
73. Vanoverschelde J-LJ, Melin JA, Bol A, Vanbutsele R, Cogneau M, Labar D, Robert A, Michel C, Wijns W. Regional oxidative metabolism in patients after recovery from reperfused anterior myocardial infarction: relation to regional blood flow and glucose uptake. *Circulation* 1992; 85:9–21.
74. Czernin J, Porenta G, Brunken R, Krivokapich J, Chen K, Bennett R, Hage A, Fung C, Tillisch J, Phelps ME, Schelbert HR. Regional blood flow, oxidative metabolism, and glucose utilization in patients with recent myocardial infarction. *Circulation* 1993; 88:884–895.
75. Kalff V, Hicks RJ, Hutchins G, Topol E, Schwaiger M. Use of carbon-11 acetate and dynamic positron emission tomography to assess regional myocardial oxygen consumption in patients with acute myocardial infarction receiving thrombolysis or coronary angioplasty. *Am J Cardiol* 1993; 71:529–535.
76. Hicks RJ, Melon P, Kalff V, Wolfe E, Dick RJ, Popma JJ, Topol E, Schwaiger M. Metabolic imaging by positron emission tomography early after myocardial infarction as a predictor of recovery of myocardial function after reperfusion. *J Nucl Cardiol* 1994; 1:124–137.
77. Henes CG, Bergmann SR, Perez JE, Sobel BE, Geltman EM. The time course of restoration of nutritive perfusion, myocardial oxygen consumption, and regional function after coronary thrombolysis. *Coron Artery Dis* 1990; 1:687–696.
78. Vanoverschelde J-LJ, Wijns W, Depre C, Essamri B, Heyndrickx GR, Borgers M, Bol A, Melin JA. Mechanisms of chronic regional postischemic dysfunction in humans: new insights from the study of noninfarcted collateral-dependent myocardium. *Circulation* 1993; 87:1513–1523.

79. Gerber BL, Wijns W, Vanoverschelde JL, Heyndrickx GR, De Bruyne B, Bartunek J, Melin JA. Myocardial perfusion and oxygen consumption in reperfused noninfarcted dysfunctional myocardium after unstable angina: direct evidence for myocardial stunning in humans. *J Am Coll Cardiol* 1999; 34:1939–1946.
80. Janier MF, Andre-Fouet X, Landais P, Gregoire MC, Lavenne F, Amaya J, Mercier C, Machecourt J, Cinotti L. Perfusion-MVO_2 mismatch during inotropic stress in CAD patients with normal contractile function. *Am J Physiol* 1996; 271:H59–H67.
81. Ohte N, Hashimoto T, Iida A, Narita N, Akita S. Extent of myocardial damage in regions with reverse redistribution at 3 h and at 24 h on ^{201}Tl SPET: evaluation based on regional myocardial oxidative metabolism. *Nucl Med Commun* 1998; 19:1081–1087.
82. Gropler RJ, Siegel BA, Sampathkumaran K, Perez JE, Sobel BE, Bergmann SR, Geltman EM. Dependence of recovery of contractile function on maintenance of oxidative metabolism after myocardial infarction. *J Am Coll Cardiol* 1992; 19:989–997.
83. Gropler RJ, Geltman EM, Sampathkumaran K, Perez JE, Moerlein SM, Sobel BE, Bergmann SR, Siegel BA. Functional recovery after coronary revascularization for chronic coronary artery disease is dependent on maintenance of oxidative metabolism. *J Am Coll Cardiol* 1992; 20:569–577.
84. Conversano A, Walsh JF, Geltman EM, Perez JE, Bergmann SR, Gropler RJ. Delineation of myocardial stunning and hibernation by positron emission tomography in advanced coronary artery disease. Am Heart J 1996; 131:440–450.
85. Hata T, Nohara R, Fujita M, Hosokawa R, Lee L, Kudo T, Tadamura E, Tamaki N, Konishi J, Sasayama S. Noninvasive assessment of myocardial viability by positron emission tomography with ^{11}C-acetate in patients with old myocardial infarction. Usefulness of low-dose dobutamine infusion. *Circulation* 1996; 94:1834–1841.
86. Gropler RJ, Geltman EM, Sampathkumaran K, Perez JE, Schechtman KB, Conversano A, Sobel BE, Bergmann SR, Siegel BA. Comparison of carbon-11-acetate with fluorine-18-fluorodeoxyglucose for delineating viable myocardium by positron emission tomography. *J Am Coll Cardiol* 1993; 22: 1587–1597.
87. Rubin PJ, Soo Lee D, Dávila-Román VG, Geltman EM, Schechtman KB, Bergmann SR, Gropler RJ. Superiority of C-11 acetate compared with F-18 fluorodeoxyglucose in predicting myocardial functional recovery by positron emission tomography in patients with acute myocardial infarction. *Am J Cardiol* 1996; 78:1230–1235.
88. Lee HH, Dávila-Román VG, Ludbrook PA, Courtois M, Walsh JF, Delano DA, Rubin PJ, Gropler RJ. Dependency of contractile reserve on myocardial blood flow: implications for the assessment of myocardial viability with dobutamine stress echocardiography. *Circulation* 1997; 96:2884–2891.
89. Wolpers HG, Burchert W, van den Hoff J, Weinhardt R, Meyer G-J, Lichtlen PR. Assessment of myocardial viability by use of ^{11}C-acetate and positron emission tomography. Threshold criteria of reversible dysfunction. *Circulation* 1997; 95:1417–1424.
90. Hicks RJ, Savas V, Currie PJ, Kalff V, Starling M, Bergin P, Kirsch M, Schwaiger M. Assessment of myocardial oxidative metabolism in aortic valve disease using positron emission tomography with C-11 acetate. *Am Heart J* 1992; 123:653–664.
91. Hicks RJ, Kalff V, Savas V, Starling MR, Schwaiger M. Assessment of right ventricular oxidative metabolism by positron emission tomography with C-11 acetate in aortic valve disease. *Am J Cardiol* 1991; 67:753–757.
92. Tadamura E, Tamaki N, Matsumori A, Magata Y, Yonekura Y, Nohara R, Sasayama S, Yoshibayashi M, Kamiya T, Konishi J. Myocardial metabolic changes in hypertrophic cardiomyopathy. *J Nucl Med* 1996; 37:572–577.
93. Ishiwata S, Maruno H, Senda M, Toyama H, Nishiyama S, Seki A. Mechanical efficiency in hypertrophic cardiomyopathy assessed by positron emission tomography with carbon 11 acetate. *Am Heart J* 1997; 133:497–503.
94. Ishiwata S, Maruno H, Senda M, Toyama H, Nishiyama S, Seki A. Myocardial blood flow and metabolism in patients with hypertrophic cardiomyopathy – a study with carbon-11 acetate and positron emission tomography. *Jpn Circ J* 1997; 61:201–210.
95. Beanlands RS, Bach DS, Raylman R, Armstrong WF, Wilson V, Montieth M, Moore CK, Bates E, Schwaiger M. Acute effects of dobutamine on myocardial oxygen consumption and cardiac efficiency measured using carbon-11 acetate kinetics in patients with dilated cardiomyopathy. *J Am Coll Cardiol* 1993; 22:1389–1398.
96. Beanlands RS, Armstrong WF, Hicks RJ, Nicklas J, Moore C, Hutchins GD, Wolpers HG, Schwaiger M. The effects of afterload reduction on myocardial carbon 11-labeled acetate kinetics and noninvasively estimated mechanical efficiency in patients with dilated cardiomyopathy. *J Nucl Cardiol* 1994; 1:3–16.
97. Bach DS, Beanlands RS, Schwaiger M, Armstrong WF. Heterogeneity of ventricular function and myocardial oxidative metabolism in nonischemic dilated cardiomyopathy. *J Am Coll Cardiol* 1995; 25:1258–1262.
98. Bengel FM, Permanetter B, Ungerer M, Nekolla S, Schwaiger M. Non-invasive estimation of myocardial efficiency using positron emission tomography and carbon-11 acetate – comparison between the normal and failing human heart. *Eur J Nucl Med* 2000; 27:319–326.
99. Torizuka T, Tamaki N, Kasagi K, Misaki T, Kawamoto M, Tadamura E, Magata Y, Yonekura Y, Mori T, Konishi J. Myocardial oxidative metabolism in hyperthyroid patients assessed by PET with carbon-11-acetate. *J Nucl Med* 1995; 36:1981–1986.
100. Hattori N, Tamaki N, Kudoh T, Masuda I, Magata Y, Kitano H, Inubushi M, Tadamura E, Nakao K, Konishi J. Abnormality of myocardial oxidative metabolism in noninsulin-dependent diabetes mellitus. *J Nucl Med* 1998; 39:1835–1840.
101. Hutchins GD, Chen T, Carlson KA, Fain RL, Winkle W, Vavrek T, Mock BH, Zipes DP. PET imaging of oxidative metabolism abnormalities in sympathetically denervated canine myocardium. *J Nucl Med* 1999; 40:846–853.
102. Bengel FM, Ueberfuhr P, Nekolla S, Ziegler SI, Reichart B, Schwaiger M. Oxidative metabolism of the transplanted human heart assessed by positron emission tomography using C-11 acetate. *Am J Cardiol* 1999; 83:1503–1505.
103. Rechavia E, De Silva R, Kushwaha SS, Rhodes CG, Araujo LI, Jones T, Maseri A, Yacoub MH. Enhanced myocardial ^{18}F-2-fluoro-2-deoxyglucose uptake after orthotopic heart transplantation assessed by positron emission tomography. *J Am Coll Cardiol* 1997; 30:533–538.